

Synthesis and Charaterization of Poly (Flouroaniline)/Mwcnt Composites

Bijaya kumar Parija¹, Chita Ranjan Biswal¹, Prasanna Kumar Sahoo², Matru Prasad Dash¹, Munesh Chandra Adhikary³, P.L.Nayak¹

1. Center of Excellence of Nanoscience and Engineering Synergy Institute of Technology, Bhipur, Phulnakhara. - 752101

2. Orissa Engineering College, Bhubaneswar-752050

3. Fakir Mohan University, Balasore-756001

Abstract

Polyfluoroaniline (poly(FAn))/carboxylic acid-functionalized multiwalled carbon nanotubes (c-MWCNTs) nanocomposites were prepared by insitu polymerization method using ammonium persulfate (APS) as an oxidant. Scanning electron microscopy (SEM) and transmission electron microscopy (TEM) showed that a tubular layer of Poly(FAn) was coated on the surface of carbon nanotubes with a thickness of 10–20 nm. Ultraviolet-visible spectroscopy (UV-vis) and Fourier transmission infrared spectroscopy (FTIR) analysis provided an evidence for the formation of nanocomposites. The thermal stability of nanocomposites was improved by addition of c-MWCNTs as confirmed by thermogravimetric analysis (TGA). XRD spectra showed that the crystalline nature of Poly(FAn) was not affected much by the addition of c-MWCNTs. As the content of c-MWCNTs was increased, the electrical conductivity of the nanocomposites increased due to the interaction between polymer and nanotubes that enhances electron delocalization.

Keywords: Fluoroaniline; multi-walled carbon nanotube; nanocomposite; oxidative polymerization.

Date of Submission: 17, December, 2012



Date of Publication: 11, January 2013

II. Introduction

In recent years, two classes of organic materials like conducting polymers and carbon nanotubes (CNTs) have gained great interest for their unique physical and chemistry properties [1-4]. An interesting application can be the embedding of little quantity of CNTs, either single-walled carbon nanotubes (SWNTs) or multi-walled carbon nanotubes (MWNTs), inside the polymer matrix of conducting polymers for the fabrication of nanocomposites [5,6]. This method of synthesis, carried on by polymerizing the monomer in the presence of a dispersion of CNTs, is very simple. Polyaniline derivatives have been deeply studied among conducting polymers in the last decades for their good electrical properties, easy methods of synthesis and high environmental stability [7e 10]. The chemistry of polyanilines is generally more complex with respect to other conducting polymers, due to their dependence on both the pH value and the oxidation states, described by three different forms known as leucoemeraldine base (fully reduced form), emeraldine base (EB) (50% oxidized form), and pernigraniline base (fully oxidized form). The most important is the EB form and its protonation by means of H⁺ ions, generated from protic acids, gives the emeraldine salt form, responsible of the strong increment of the conducting properties [11]. This process is reversible and it is possible for the presence of imine group basic sites located along the conducting polymer backbone [12,13]. The doping process of polyanilines is always associated to conformational modifications of the polymer chains, due to the local distortions created by the addition of H⁺ ions to the basic sites [14]. These distortions are even able to affect the morphology of the deposited films by varying their organization and play an important role in the electrical properties of the conducting polymer [15]. The number and kind of substituents along the aromatic rings of the polymer backbone seems to affect the molecular rearrangement occurring during the doping process and in some cases, the sterical hindrance generated by “too close” substituents to the aromatic ring is responsible of the spontaneous undoping process [16]. Taking into account these considerations, the aim of the present study was to investigate the possible variations on polyaniline derivatives physical chemistry properties by performing standardized oxidative polymerizations on monomers with different kind and number of substituents along the aromatic rings.

Recently Wang et. al. [17] have synthesized chlorinated polyaniline and found that it is soluble in THP both in doped and undoped form. Chemical synthesis and successful polymerization of poly (fluoroaniline) has been accomplished [18]. The synthesis of different homopolymers and copolymers derived from anilines bearing electron withdrawing groups has been reported. The electrochemical polymerization of halogen-substituted anilines was carried out and have been reported the copolymerizations of aniline with monoortho-

halogenated anilines (2-fluoroaniline), and they showed that the presence of fluorine-substituted groups in the ortho position did not adversely affect the polymerization. Therefore halo derivative of polyaniline has been synthesized in order to enhance its solubility in solvent. A survey of the literature reveals that poly(fluoro anilines) have not been imbedded with MWCNT to study its properties .

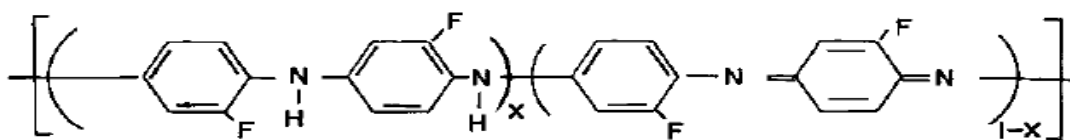


Figure.1 Structure of polyfluoroaniline.

In the present research program , attempt has been made to synthesize and characterize the poly(FAn) with MWNT fabricated by in situ polymerization. The entanglement of fluorine in the matrix might enhance various properties of the substrate The nanocomposites were characterized by a number of techniques including ultraviolet (UV)–visible, Fourier transform infrared spectroscopy (FTIR), scanning electron microscopy (SEM), transmission electron microscopy (TEM), X-ray diffraction (XRD), and electrical conductivity.

III. Work-Up Procedure

Materials

Flouroaniline and aniline monomers were purchased from Aldrich. Multi-walled CNT (90% purification) used in this study was purchased from Cheap Tubes (USA, 10– 20 nm diameter). Other reagents like ammonium persulfate (APS), hydrochloric, sulfuric, and nitric acid (Sigma Chemicals) were of analytical grade.

Oxidation of MWNT

MWNTs were suspended in a 3:1 mixture of concentrated H₂SO₄ and HNO₃ and refluxed for 30 min in an ultrasonic bath. The solution was magnetically stirred and heated at 60⁰C for 24 h. This treatment provides carboxylic acid groups at defects in the surface of tubes and exfoliates graphite. The obtained c-MWNTs were filtered through 0.2-μm polytetrafluoroethylene (PTFE) membrane filter, washed with plenty of deionized water until the pH value was around 7, and then dried at 70⁰C for 24 h.

Synthesis of Poly(FAn)/c-MWCNT polymer composites

Poly(FAn) /c-MWCNT composites were synthesized by in situ chemical oxidative polymerization method. In a typical experiment, various weight ratios of c-MWCNTs were dissolved in 80 mL 1.2 M hydrochloric acid solutions and ultrasonicated over 2 h, transferred into a 250-mL beaker ,2.80mL of aniline and 2.90 mL of flouroaniline were added to the above c-MWCNT suspension [185]. Subsequently 50 mL of a 1.2 M HCl solution containing 12.5 g of APS was added into the suspension with constant mechanical stirring at room temperature. The reaction mixture was stirred for a further 12 h, and then filtered. The remaining filter cake was rinsed several times with distilled water and ethanol. The powder thus obtained was dried under vacuum at 60⁰C for 24 h. The % of c-MWCNT used was 0, 2, 5 %.Schematic drawing of the mechanism governing the formation of Poly(FAn)/c-MWCNT composites is shown in the figure 2.

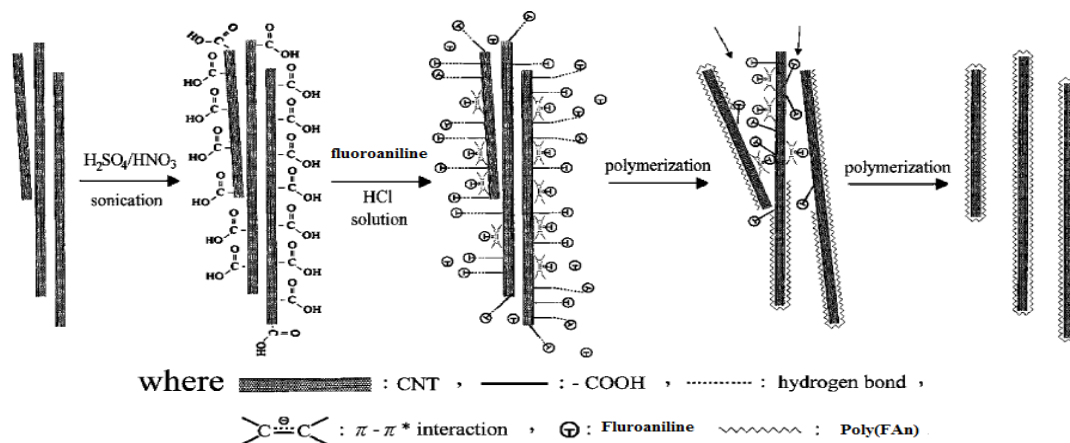


Figure.2. Schematic drawing of the mechanism governing the formation of Poly(FAn)/c-MW CNT composites.

IV. Measurement

UV-vis absorption spectra measurement

All the UV-vis measurements were performed using a Shimadzu PC3101 spectrophotometer, under computer control.

IR spectra

The Fourier transform infrared (FT-IR) spectra were recorded on a Nicolet 8700 spectrometer, in the range 400–4,000 cm^{-1} .

SEM

Morphology of the Poly(FAn)/c-MWCNTS composite was investigated using a Philip XL 30 SEM at an accelerating voltage of 25 kV. The sample was fractured at liquid nitrogen temperature and then was coated with a thin layer of gold before observation.

TEM

TEM experiments were performed on a Hitachi H-8100 electron microscope with an acceleration voltage of 200 kV.

XRD

X-ray diffraction (Rigaku, D/Max, 2,500 V, Cu- α radiation: 1.54056 \AA) experiments were carried out on both the plain PAA and the composite samples. Wide-angle X-ray diffractograms were recorded at temperature of 30 $^{\circ}$ C after isothermal crystallization at this temperature for 1 h .

TGA

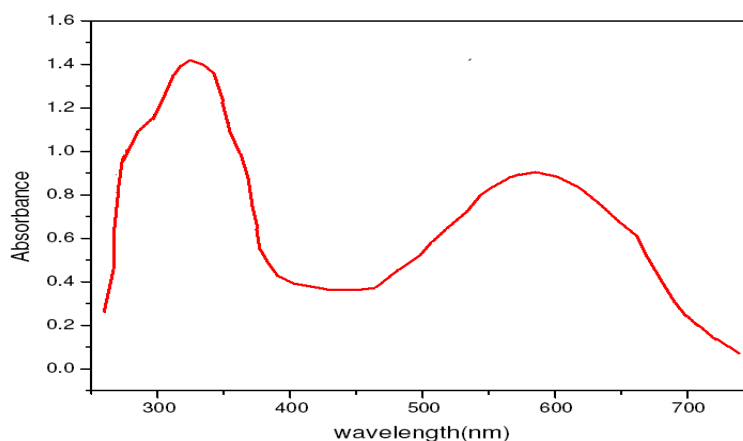
TGA studies were performed on a TA instrument (SDT Q600 analyzer) from 30 $^{\circ}$ C to 800 $^{\circ}$ C at a heating rate of 10 $^{\circ}$ C/min under nitrogen atmosphere.

Conductivity

The standard Van Der Pauw DC four-probe method was used to measure the electron transport behaviors of Poly(FAn) and Poly(FAn)/c-MWCNT composites. The samples of Poly(FAn) and Poly(FAn)/c-MWCNTs were pressed into pellet. The pellet was cut into a square. The square was placed on the four probe apparatus, providing a voltage for the corresponding electrical current could be obtained. The electrical conductivity of samples was calculated by the following formula: σ (S/cm) = $(2.44 \times 10/S) \times (I/E)$, where r is the conductivity, S the sample side area, I the current passed through outer probes, and E the voltage drop across inner probes.

4.1 Results and discussion

4.2. UV



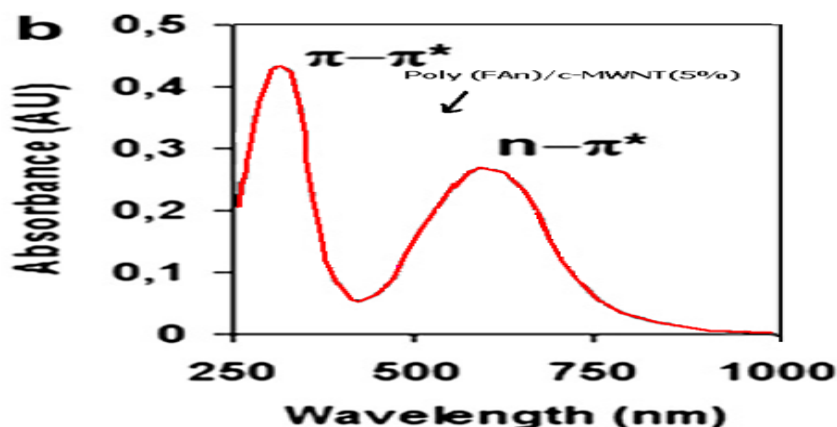


Figure.3. UV-vis of (a) Bare polymer (b) Poly(FAn)/c-MWCNT(5%)

The UV-vis spectra of the poly(FAn) and poly(FAn)/c-MWNTs composites in NMP solutions are presented in Figure 3. Due to deprotonation effects of NMP, the spectra are similar with that of Poly(FAn) (Figure 3a). The major peak at about 316 and 618 nm is observed, which are assigned to the excitation of the benzene and quinoid segments on the polyemeraldine chain, respectively. In case of Poly(FAn)/c-MWNT absorption peaks at 320, 820 nm are formed, shown in the Figure 3.41(b). The absorption peak at about 320 nm can be ascribed to $\pi-\pi^*$ transition of the benzenoid rings, whereas the peaks at around 410 and 820 nm can be attributed to polaron- π^* and π -polaron transition, respectively.

4.3. FTIR of the composites.

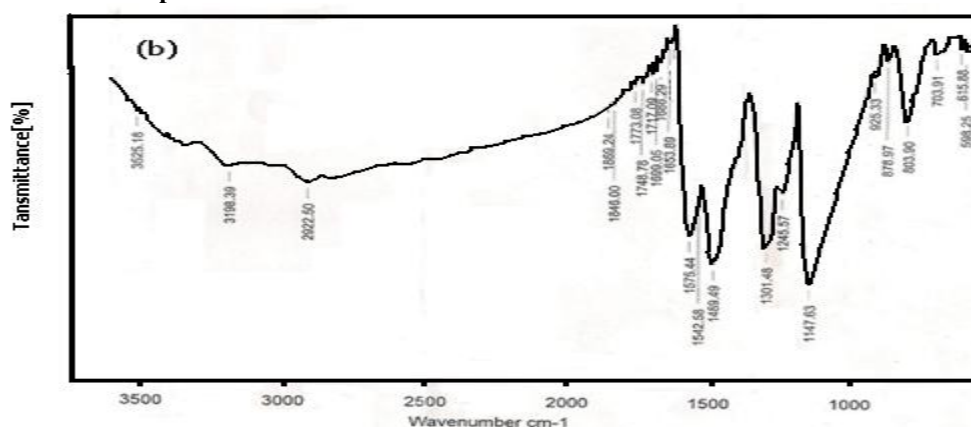


Figure.4. FT-IR data of Poly(FAn)/c-MWCNT(5%)

The FTIR spectra used to characterize the structure of bare polymer and Poly(FAn)/c-MWNT composites are presented in the Figure 4. The FTIR spectra for the Poly(FAn)/c-MWNT(5%) shows the characteristic peaks at 3525, 1575, 1489, 1301, 1245, 1147 and 803 cm^{-1} , respectively. The peak at 1575 cm^{-1} is due to C=C double bond of quinoid rings, whereas the peak at 1489 cm^{-1} arises due to vibration of C=C double bond associated with the benzenoid ring. The peak at 1301 cm^{-1} has been attributed to a combination of C-N in quinoid and benzenoid sequences. In addition, the band appearing at 703 cm^{-1} probably corresponds to the C-H out-of-plane bending vibration of the 1,2,3-trisubstituted benzene rings. The absorption peak observed at 1128 cm^{-1} has been associated with the presence of halogen (fluoro) group in the copolymer. The presence of carboxylic acid groups due to c-MWNT was confirmed with a C=O band stretching that appears around 1,699 cm^{-1} , whereas the band at 1,147 cm^{-1} is attributed to the C-O stretching vibrations of -COOH groups.

4.4.XRD

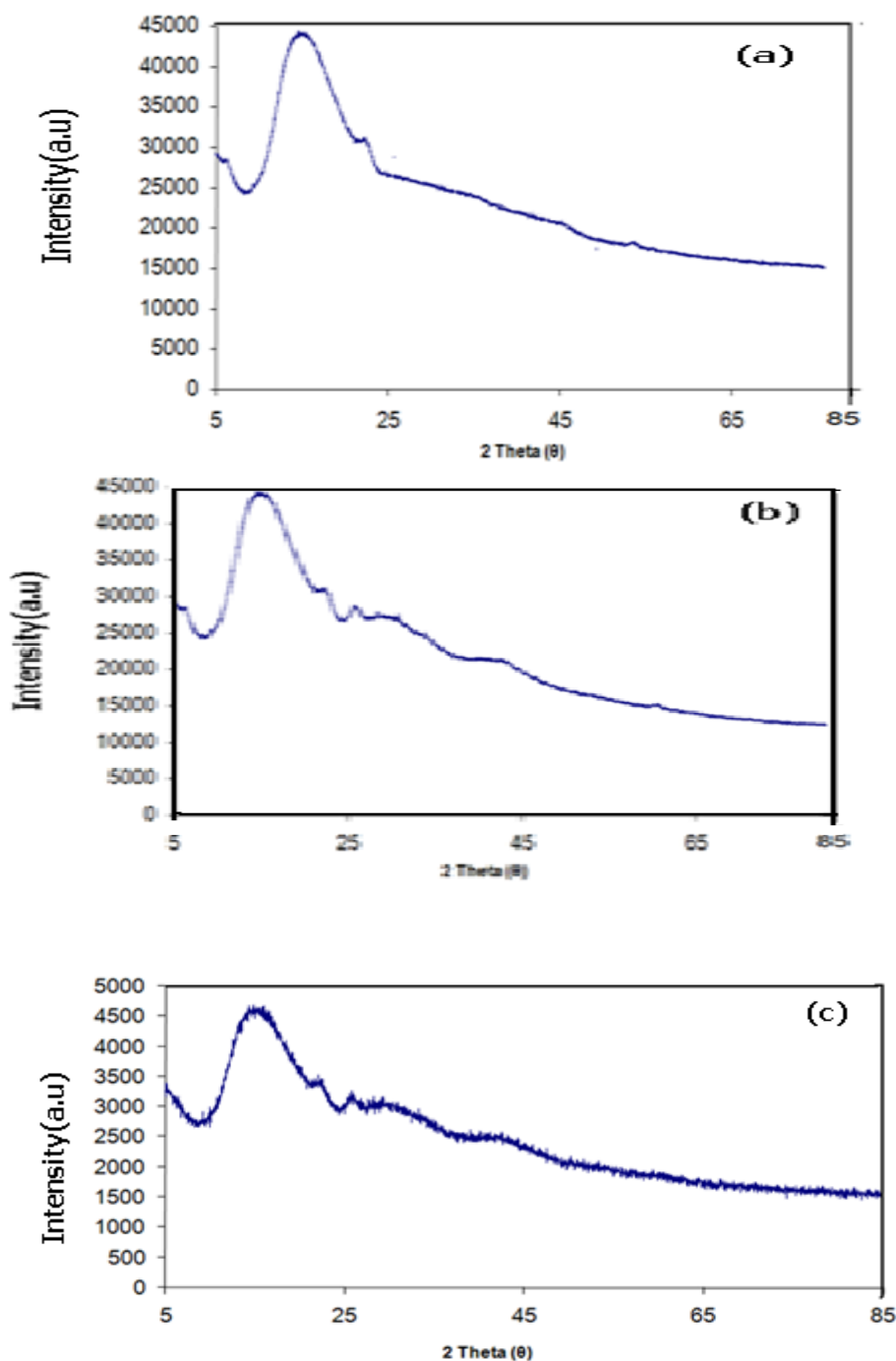


Figure.5. XRD datas of (a)Bare Polymer(b)Poly(FAn)/c-MWCNT(2%)(c)Poly(FAn)/c-MWCNT(5%)

The structural characteristics of Poly(FAn)/MWNT composites were analyzed by XRD measurements, shown in the figure.5. The XRD patterns of c-MWNTs (25.7°, 42.8°). In contrast, composites show a different structural order. Besides the XRD patterns of MWNT (peaks at 27.8° and 43.0°), additional structural order can be seen through the appearance of peaks at 18.5° and 20.9° due to the presence of Poly(FAn). This type of induction of additional structural ordering was witnessed in composites of c-MWNT with other polymers. This may arise from strong $\pi-\pi^*$ interactions between Poly(FAn) and MWNT.

4.5.SEM

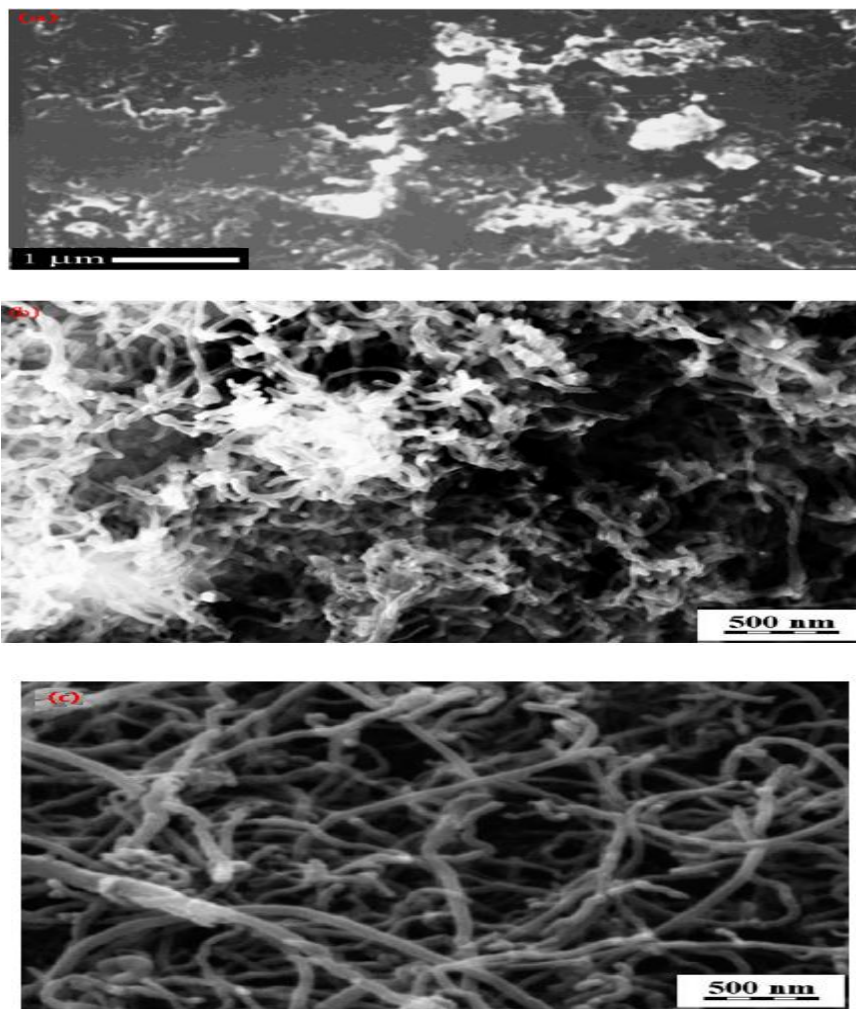
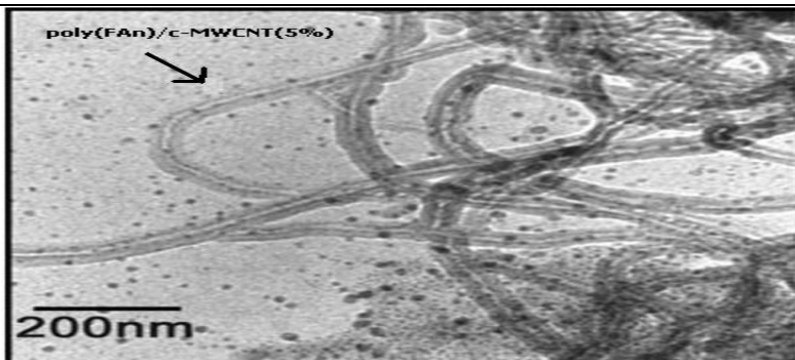


Figure.6. SEM image of (a) bare Polymer(b)Poly(FAn)/c-MWCNT(2%)(c)Poly(FAn)/c-MWCNT(5%)

SEM micrographs of the bare polymer and nanocomposite with 5% c-MWCNTs are shown in figure 6. SEM images clearly showed that there were two different types of material to be visible: the thinner fibrous phase and the larger block phase. With the increasing of c-MWNTs, more and more individual fibrous phases were formed (Fig. 3). The diameters of the individual fibrous phases ranged from several tens to hundreds of nanometers, depending on the PNMA content. The diameters of the individual fibrous phases became larger than that of the original c-MWNTs (diameter 20–30 nm) after in situ polymerization, and therefore the carbon nanotubes must be coated by a Poly(FAn) layer.

4.6.TEM



The TEM image of Poly(FAn)/c-MWCNT is shown in the Figure.3.46. The apparent physical nature of the copolymer changed remarkably after nanocomposite formation and clearly shows the core-shell structure. The co monomer molecules are uniformly polymerized on the surface of c-MWCNTs and form a tubular nanocomposite. The diameter of the nanocomposite becomes larger than that of the c-MWCNTs after polymerization. From the figure it was clearly shows that the c-MWCNTs are well wrapped by the copolymer. SEM and TEM images, we conclude that c-MWCNTs are well dispersed in the copolymer matrix.

4.7.TGA

Figure.3.46. TEM image of Poly(FAn)/c-MWCNT(5%)

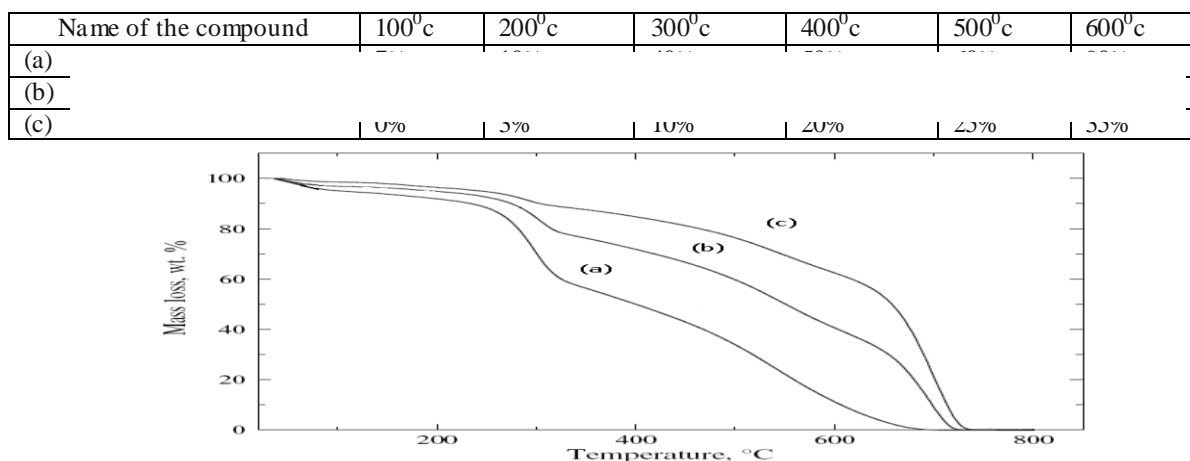


Figure3.47. TGA data of (a)Bare Polymer(b)Poly (FAn)/c-MWCNT(2%)(c)Poly(FAn)/c-MWCNT(5%)

Table-1.Weight loss at different temperature

The degradation pattern of the (a)neat polymer,(b)poly(FAn)/c-MWCNT(2%) and (c)poly(FAn)/c-MWCNT(5%) are given in the figure and the results summarized in the table-1.The perusal of the figure indicates that at 100⁰c weight loss in case of neat polymer is around 7% ,for the sample (b) it is around 5% and for the sample (c) it is 0%.At 200⁰c weight loss for the neat polymer ,sample(b) and sample(c) is around 10%,5% and 3%.At 300⁰c the weight loss for the neat polymer ,sample (b) and sample(c) is around 40%,20% and 10% respectively. At 600⁰c the weight loss is 90%,60% and 35% for neat polymer, sample (a)and sample(c) respectively .The weight loss between 100-200⁰c is around 10%.This may be due to the absorbance of water vapour by the sample. In case of neat polymer the weight loss is 50% at 400⁰c and 60% at 500⁰c this may be due to the breakage of carbon fluorine bond present in the polymer. Further it is absorbed that if weight percent of c-MWCNT increases the compound become more and more strong resist degradation.This is ascertained fact that at 600⁰c the weight loss for the sample (b) is 60% where as for the sample(c) the weight loss is 35% hence it can be concluded that incorporation of CNT the material become more and more strong and resists degradation.

4.8. Conductivity.

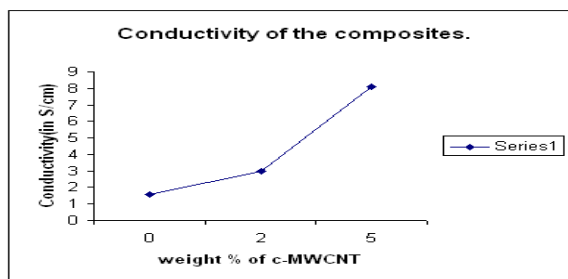


Figure.3.48. Conductivity data of Poly(FAn)/c-MWCNT composites.

Room temperature conductivity of the copolymer and nanocomposites varies over a range from 1.58×10^{-8} S/cm to 8.5×10^{-4} S/cm. The conductivity of copolymer poly (FAn) prepared in situ polymerization method was found to be 3.12×10^{-2} S/cm. The conductivity of nanocomposites increases depending on the feed ratio of the c-MWCNTs. With the addition of 2% of c-MWCNTs, the conductivity increases by one order of magnitude (3×10^{-7} S/cm), and with the addition of 5% c-MWCNTs, the conductivity increases up to 8.5×10^{-4} S/cm. The reason for improvement in conductivity is the π - π^* interaction between the surface of c-MWCNTs and the quinoid ring of the copolymer chain which effectively improves the degree of electron delocalization between the two components, as confirmed by FT-IR and UV-visible spectra. Moreover, it can be attributed to the more ordered chain conformation of the copolymer.

V. Conclusion.

Poly(FAn)/c-MWCNTs nanocomposites were successfully synthesized via in situ emulsion polymerization. The results conclude that there is a "binder" between MWCNTs and copolymer, where copolymer wrapped completely on the surface of the carbon nanotubes. SEM and TEM measurement proved that the c-MWCNTs were homogeneously dispersed in the copolymer matrix. The interaction between c-MWCNTs and copolymer chain was confirmed by FT-IR and UV-visible spectra. The nanocomposites showed higher thermal stabilities in comparison with the bare copolymer. Room temperature conductivity of nanocomposite increased to one order of magnitude with the addition of 5% c-MWCNTs. The highly ordered structures of nanocomposites were confirmed by XRD patterns. The method reported herein is a simple, effective, and inexpensive route for synthesizing poly(FAn)/c-MWCNT nanocomposites. In addition, the versatility of this method could be extended to prepare other polymer/CNT nanocomposites by choosing appropriate experimental conditions.

References

- [1]. MacDiarmid AG, Yang LS, Huang WS, Humphrey BD. *Synth Met* 1987;18:393.
- [2]. Iijima S. *Nature* 1991;56:354.
- [3]. Dresselhaus MS, Dresselhaus G, Eklund PC. *Science of fullerenes and carbon nanotubes*. New York: Academic Press; 1996.
- [4]. Iijima S, Brabec C, Maiti A, Bernholc JJ. *Chem Phys* 1996;5:2089.
- [5]. Coleman JN, Curran S, Dalton AB, Davey AP, McCarthy B, Blau W, et al. *Phys Rev B* 1998;58:7492.
- [6]. Bavastrello V, Ram MK, Nicolini C. *Langmuir* 2002;20:1535.
- [7]. MacDiarmid AG, Chiang JC, Halpen M, Huang WS, Mu SL, Somasiri NLD, et al. *Mol Cryst Liq Cryst* 1985;121:173.
- [8]. Paul EW, Ricco AJ, Wrighton MSJ. *Phys Chem* 1985;89:1441.
- [9]. Epstein AJ, MacDiarmid AG. In: Kuzmany H, Mehring M, Roth S, editors. *Electronic properties of conjugated polymer*. Berlin: Springer-Verlag; 1989.
- [10]. Kobayashi T, Yoneyama H, Tamura HJ. *Electroanal Chem* 1984;177:281.
- [11]. Chiang JC, MacDiarmid AG. *Synth Met* 1986;13:193.
- [12]. Epstein AJ, Ginder JM, Zuo F, Bigelow RW, Woo HS, Tanner DB, et al. *Synth Met* 1987;18:303.
- [13]. Genies EM, Labkowski MJ. *Electroanal Chem* 1987;236:199.
- [14]. de Oliveira Jr ZT, dos Santos MC. *Solid State Commun* 2000;114:49.
- [15]. Bavastrello V, Erokhin V, Carrara S, Sbrana F, Ricci D, Nicolini C. *Thin Solid Films* 2004;468:17.
- [16]. Bavastrello V, Stura E, Carrara S, Erokhin V, Nicolini C. *Sensors Actuators B* 2004;98:247.
- [17]. X.H. Wang, L.X. Wang, X.B. Jing, F.S. Wang, *Synth. Metals* **69**, 149(1995).
- [18]. A.H. Kwon, J.A. Conkin, M.Makhinson, R.B. Kaner, *Synth. Metal* **84**, 95 (1997)